ISSN 1070-3284, Russian Journal of Coordination Chemistry, 2021, Vol. 47, No. 12, pp. 915–921. © Pleiades Publishing, Ltd., 2021.

Syntheses, Structural Characterization of Two Cobalt Coordination Polymers Composed of Isophthalate and Bis(4-(1*H*-imidazol-1-yl)phenyl)methanone Ligands

G. F. Wang[a], * and S. W. Sun[a]

[a] *Department of Applied Chemistry, Yuncheng University, Yuncheng, 044000 P.R. China*

**e-mail: wgf1979@126.com*

Received June 8, 2021; revised June 23, 2021; accepted June 24, 2021

Abstract—Two 2D cobalt complexes, namely $\{[(\mathrm{Bipmo})_2\mathrm{Co}_2(\mathrm{Ipa})_2](\mathrm{DMF})]\cdot 2.25\mathrm{H}_2\mathrm{O}\}_n$ (**I**), $\{[(\mathrm{Bipmo})\mathrm{Co}(\mathrm{Ipa})]\cdot 2\mathrm{H}_2\mathrm{O}\}_n$ (**II**), have been constructed solvothermally using isophthalic acid (H_2Ipa), bis(4-(1*H*-imidazol-1-yl)phenyl)methanone (Bipmo), and cobalt acetate at different temperatures. Single-crystal X-ray diffraction analyses (CIF files CCDC nos. 2078773 (**I**), 2078774 (**II**)) reveal that **I** and **II** crystallize in the triclinic and monoclinic systems, space groups $P\bar{1}$, and $P2_1/c$, respectively. Complex **I** presents a 2D uninodal network with the point symbol $\{4^4\cdot 6^2\}$ along [1 1 –1] direction, while complex **II** shows two fold interpenetration with the same point symbol.

Keywords: coordination polymers, semirigid ligand, topology, cobalt complex, X-ray crystallography

DOI: 10.1134/S1070328421120034

INTRODUCTION

Over the past few decades, crystalline coordination polymers (CPs) have attract much attention not only because of their intriguing structural variety of architectures and topologies, but also because of their potential applications in catalysis, ion exchange, sorption, luminescence, magnetism, and so on [1–6]. Although chemists have devoted much effort to the construction of new coordination polymers, it is still a daunting task to predict or modulate crystalline coordination polymers, because the final structures are often governed by many delicate factors, such as solvents, temperature, pH values, metal ions, and the structural features of organic ligands [1–9]. Besides, the structural diversity can be found as a result of isomerism and entanglement. Interpenetration, which challenges our knowledge in design and synthesis of CPs, is an approach of the nature to avoid open space or the voids in a network.

In our previous work, N-donor V-shaped bidentate ligands, such as bis(4-(1*H*-imidazol-1-yl)phenyl)methanone and bis(4-(2'-methylimidazol)phenyl)sulfone are chosen as ancillary ligands [6–11]. Going further with our previous work, we reported here two novel CPs based on bis(4-(1*H*-imidazol-1-yl)phenyl)methanone (Bipmo) and isophthalic acid (H_2Ipa) (Scheme 1), namely $\{[(\mathrm{Bipmo})_2\mathrm{Co}_2(\mathrm{Ipa})_2](\mathrm{DMF})]\cdot 2.25\mathrm{H}_2\mathrm{O}\}_n$ (**I**), $\{[(\mathrm{Bipmo})\mathrm{Co}(\mathrm{Ipa})]\cdot 2\mathrm{H}_2\mathrm{O}\}_n$ (**II**). The complexes were characterized by IR spectra, elemental analyses, and X-ray crystallography.

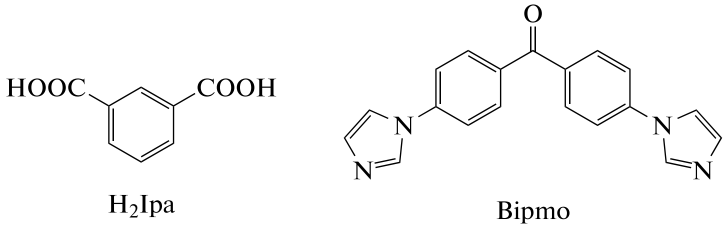

Scheme 1.

EXPERIMENTAL

Materials and measurements. All reagents were purchased as analytical grade and used without further purification. Bipmo was synthesized according to the literature [12]. Elemental analyses were performed on an Elementar Vario ELIII elemental analyzer. IR spectra were recorded on a Bruker Vector 22 spectrophotometer with KBr pellets in the 4000–400 cm^{-1} region.

Synthesis of $\{[(Bipmo)_2Co_2(Ipa)_2](DMF)]\cdot 2.25H_2O\}_n$ (I). A mixture of $Co(OAc)_2\cdot 4H_2O$ (0.1 mmol), Bipmo (0.1 mmol), H_2Ipa (0.1 mmol) and DMF and H_2O (4 and 2 mL) was added in a 15 mL Teflon-lined stainless steel reactor at 105°C for 3 days and then slowly cooled to room temperature. Blocks of single crystals were obtained by filtration, washed with H_2O and air-dried. The yield was 63% (blue, based on Bipmo).

IR (KBr; ν, cm^{-1}): 3238, 3135, 1641, 1617, 1560, 1524, 1492, 1483, 1438, 1393, 1330, 1306, 1285, 1265, 1252, 1184, 1153, 1124, 1109, 1061, 963, 931, 860, 840, 765, 740,718, 672, 649, 620, 483, 419.

For $C_{57}H_{47.50}N_9O_{13.25}Co_2$

Anal. calcd., %	C, 57.61	H, 4.03	N, 10.61
Found, %	C, 57.52	H, 3.94	N, 10.53

Synthesis of $\{[(Bipmo)Co(Ipa)]\cdot 2H_2O\}_n$ (II). A mixture of $Co(OAc)_2\cdot 4H_2O$ (0.1 mmol), Bipmo (0.1 mmol), H_2Ipa (0.1 mmol) and DMF and H_2O (4 and 2 mL) was added in a 15 mL Teflon-lined stainless steel reactor at 95°C for 4 days and then slowly cooled to room temperature. Blue blocks of single crystals were obtained by filtration, washed with H_2O, and air-dried. The yield was 58% (blue, based on Bipmo).

IR (KBr; ν, cm^{-1}): 3201, 3128, 3095, 1672, 1654, 1628, 1607, 1543, 1521, 1496, 1478, 1453, 1393, 1333, 1307, 1274, 1257, 1122, 1068, 993, 957, 929, 865, 854, 831, 768, 748, 651, 621, 558, 537, 515, 441.

For $C_{27}H_{22}N_4O_7Co$

Anal. calcd., %	C, 56.55	H, 3.87	N, 9.77
Found, %	C, 56.47	H, 3.81	N, 9.73

X-ray crystallographic studies. X-ray crystallographic data of **I** were recorded on an Agilent Technology SuperNova Eos Dual system with a (MoK_α, λ = 0.71073 Å) micro focus source and focusing multilayer mirror optics. The data were collected at a temperature of 293 K and processed using CrysAlis^{Pro} [13]. Measurements of **II** were made on a Bruker Smart-1000 CCD diffractometer equipped with a graphite-monochromatic MoK_α radiation (λ = 0.71073 Å) by using an φ and ω scans mode at 293(2) K. Absorption corrections were applied using the program SADABS [14]. The structures were solved by direct methods [15] with the SHELXTL (version 6.10) program [14, 15] and refined by full matrix least-squares techniques on F^2 with the SHELXTL [14, 15]. All non-hydrogen atoms were refined anisotropically and the hydrogen atoms bonded to carbon atoms were generated geometrically. The water hydrogen atoms were first located in the difference map then positioned geometrically and allowed to ride on their respective parent atoms, respectively. The details of crystal data and refinement for **I** and **II** are given in Table 1. Selected bond distances and angles for **I** and **II** are listed in Table 2.

Supplementary material for structures has been deposited with the Cambridge Crystallographic Data Centre (CCDC nos. 2078773 (**I**), 2078774 (**II**); deposit@ccdc.cam.ac.uk or http://www.ccdc.cam.ac.uk).

RESULTS AND DISCUSSION

Two complexes **I** and **II** can be obtained by reaction of $Co(OAc)_2$, H_2Ipa and Bipmo in moderate yields at different temperatures under solvothermal conditions. They are air-stable and insoluble in common solvents, such as CH_2Cl_2, EtOH, MeOH, H_2O, etc. Numerous parallel experiments were carried out by adjusting the ratios of the starting materials. Additionally, a series of parallel experiments to change temperatures, and to vary the solvent types and ratios were also performed. However, other experiments gave small polycrystals or powder forms. The IR spectra shows absorption bands in the region of ~1617–1438 cm^{-1} for **I** and **II**, which is characteristic of the stretching vibrations of aryl group. Additionally, the $\nu_{C=O}$ values are observed at 1641 and 1672 cm^{-1}, similar to the previously reported bis(4-(1*H*-imidazol-1-yl)phenyl)methanone ligands [6, 9–12].

Complex **I** crystallizes in a triclinic system with space group $P\bar{1}$. There are two crystallographically independent Co(II) atoms, two Ipa^{2-} ligands, two Bipmo ligands, two and a quarter lattice water molecules, and a guest DMF molecule (Fig. 1). Each Co atom has a octahedrally coordinated geometry, bonded by two oxygen atoms from two Ipa ligands in μ_1-η^0:η^1 monodentate modes and two oxygen atoms from the third Ipa ligand in μ_1-η^1:η^1 chelating mode, two nitrogen atoms from two Bipmo ligands. The Co–O bond lengths are in the range of 2.019(3)–2.331(3) Å, and OCoO angles are between 58.55(11)° and 151.89(2)°, according with other Co-containing structures. The Co–N bond lengths are in the range of 2.111(4)–2.124(4) Å with the bond angles of 177.50(14)° ($N(8)^{\#2}Co(1)N(1)$; $^{\#2}$ $x - 1, y, z - 1$), and 178.96(14)° ($N(5)Co(2)N(4)^{\#4}$; $^{\#4}$ x, $y - 1$, $z - 1$), respectively.

From a topological point of view, if two adjacent $\{Co(1)\}_2$ units and two adjacent $\{Co(2)\}_2$ acts as 4-con-

Table 1. Crystallographic data and refinement parameters for structures **I** and **II**

Temperature, K	293(2)	293(2)
Fw	1188.40	573.42
Crystal system	Triclinic	Monoclinic
Crystal size, mm	0.26 × 0.25 × 0.23	0.48 × 0.34 × 0.26
Space group	$P\bar{1}$	$P2_1/c$
a, Å	12.1767(4)	10.5719(10)
b, Å	15.1074(5)	13.2471(12)
c, Å	16.2763(5)	19.7282(16)
α, deg	91.026(3)	90
β, deg	90.492(3)	114.434(4)
γ, deg	94.351(3)	90
V, Å^3	2.9849(2)	2.5154(4)
ρ_{cacld}, g cm^{-3}	1.322	1.514
Z	2	4
μ, mm^{-1}	0.624	0.738
θ Range, deg	2.87–25.19	3.08–27.55
Reflections measured/unique (R_{int})	24241/10727 (0.0261)	38935/5780 (0.0289)
Reflections with $I > 2\sigma(I)$	8222	4805
Data/restraints/parameters	10727/24/757	5780/0/352
GOOF on F^2	1.081	1.010
R_1, wR_2 ($I > 2\sigma(I)$)	0.0579, 0.1994	0.0346, 0.0854
R_1, wR_2 (all data)	0.0747, 0.2172	0.0458, 0.0909
$\Delta\rho_{max}/\Delta\rho_{min}$, e/Å^3	0.815/–0.416	0.320/–0.329

Table 2. Selected bond lengths and angles for complex **I** and **II***

Bond	d, Å	Bond	d, Å
I			
Co(1)–O(6)	2.031(3)	Co(1)–O(1)	2.331(3)
Co(1)–O(7)$^{\#1}$	2.047(3)	Co(2)–O(3)	2.019(3)
Co(1)–N(8)$^{\#2}$	2.118(3)	Co(2)–O(4)	2.023(3)
Co(1)–O(2)	2.119(3)	Co(2)–N(5)	2.111(4)
Co(1)–N(1)	2.124(4)	Co(2)–N(4)$^{\#4}$	2.116(4)
Co(2)–O(8)$^{\#3}$	2.171(3)	Co(2)–N(4)$^{\#4}$	2.116(4)
Co(2)–O(9)$^{\#3}$	2.261(3)		
II			
Co(1)–O(4)$^{\#1}$	2.1186(16)	Co(1)–O(2)	2.0577(14)
Co(1)–O(3)$^{\#1}$	2.2809(15)	Co(1)–N(1)$^{\#2}$	2.0588(15)
Co(1)–O(1)	2.3249(14)	Co(1)–N(3)	2.0600(14)
Angle	ω, deg	Angle	ω, deg
I			
O(6)Co(1)O(7)$^{\#1}$	121.00(11)	O(3)Co(2)O(4)	118.25(12)
O(6)Co(1)N(8)$^{\#2}$	87.77(13)	O(3)Co(2)N(5)	88.98(14)
O(7)$^{\#1}$Co(1)N(8)$^{\#2}$	87.02(12)	O(4)Co(2)N(5)	90.67(16)
O(6)Co(1)O(2)	92.18(11)	O(3)Co(2)N(4)$^{\#4}$	90.16(14)
O(7)$^{\#1}$Co(1)O(2)	146.48(12)	O(4)Co(2)N(4)$^{\#4}$	89.24(16)
N(8)$^{\#2}$Co(1)O(2)	89.93(12)	N(5)Co(2)N(4)$^{\#4}$	178.96(14)
O(6)Co(1)N(1)	89.84(14)	O(3)Co(2)O(8)$^{\#3}$	151.89(12)
O(7)$^{\#1}$Co(1)N(1)	93.60(13)	O(4)Co(2)O(8)$^{\#3}$	89.86(12)
N(8)$^{\#2}$Co(1)N(1)	177.50(14)	N(5)Co(2)O(8)$^{\#3}$	90.19(14)
O(2)Co(1)N(1)	90.89(13)	N(4)$^{\#4}$Co(2)O(8)$^{\#3}$	90.85(13)
O(6)Co(1)O(1)	150.72(11)	O(3)Co(2)O(9)$^{\#3}$	93.28(11)
O(7)$^{\#1}$Co(1)O(1)	88.16(11)	O(4)Co(2)O(9)$^{\#3}$	148.40(12)
N(8)$^{\#2}$Co(1)O(1)	91.52(13)	N(5)Co(2)O(9)$^{\#3}$	92.06(14)
O(2)Co(1)O(1)	58.55(11)	N(4)$^{\#4}$Co(2)O(9)$^{\#3}$	88.57(14)
N(1)Co(1)O(1)	90.92(14)	O(8)$^{\#3}$Co(2)O(9)$^{\#3}$	58.67(10)
II			
O(2)Co(1)N(1)$^{\#2}$	118.41(6)	N(3)Co(1)O(3)$^{\#1}$	95.31(6)
O(2)Co(1)N(3)	92.77(5)	O(4)$^{\#1}$Co(1)O(3)$^{\#1}$	58.94(6)
N(1)$^{\#2}$Co(1)N(3)	99.82(6)	O(2)Co(1)O(1)	59.22(5)
O(2)Co(1)O(4)$^{\#1}$	142.63(6)	N(1)$^{\#2}$Co(1)O(1)	90.17(6)
N(1)$^{\#2}$Co(1)O(4)$^{\#1}$	88.66(6)	N(3)Co(1)O(1)	151.45(5)
N(3)Co(1)O(4)$^{\#1}$	108.35(6)	O(4)$^{\#1}$Co(1)O(1)	98.48(6)
O(2)Co(1)O(3)$^{\#1}$	89.43(6)	O(3)$^{\#1}$Co(1)O(1)	90.18(6)
N(1)$^{\#2}$Co(1)O(3)$^{\#1}$	147.26(6)		

* Symmetry transformations used to generate equivalent atoms: Symmetry codes: $^{\#1}$ $-x, -y+1, -z$; $^{\#2}$ $x-1, y, z-1$; $^{\#3}$ $-x+1, -y, -z$; $^{\#4}$ $x, y-1, z-1$; $^{\#5}$ $1-x, 1-y, 1-z$; $^{\#6}$ $x+1, y, z+1$; $^{\#7}$ $x, y+1, z+1$ (**I**); $^{\#1}$ $-x+1, y+1/2, -z+3/2$; $^{\#2}$ $-x-1, y-1/2, -z+3/2$ (**II**).

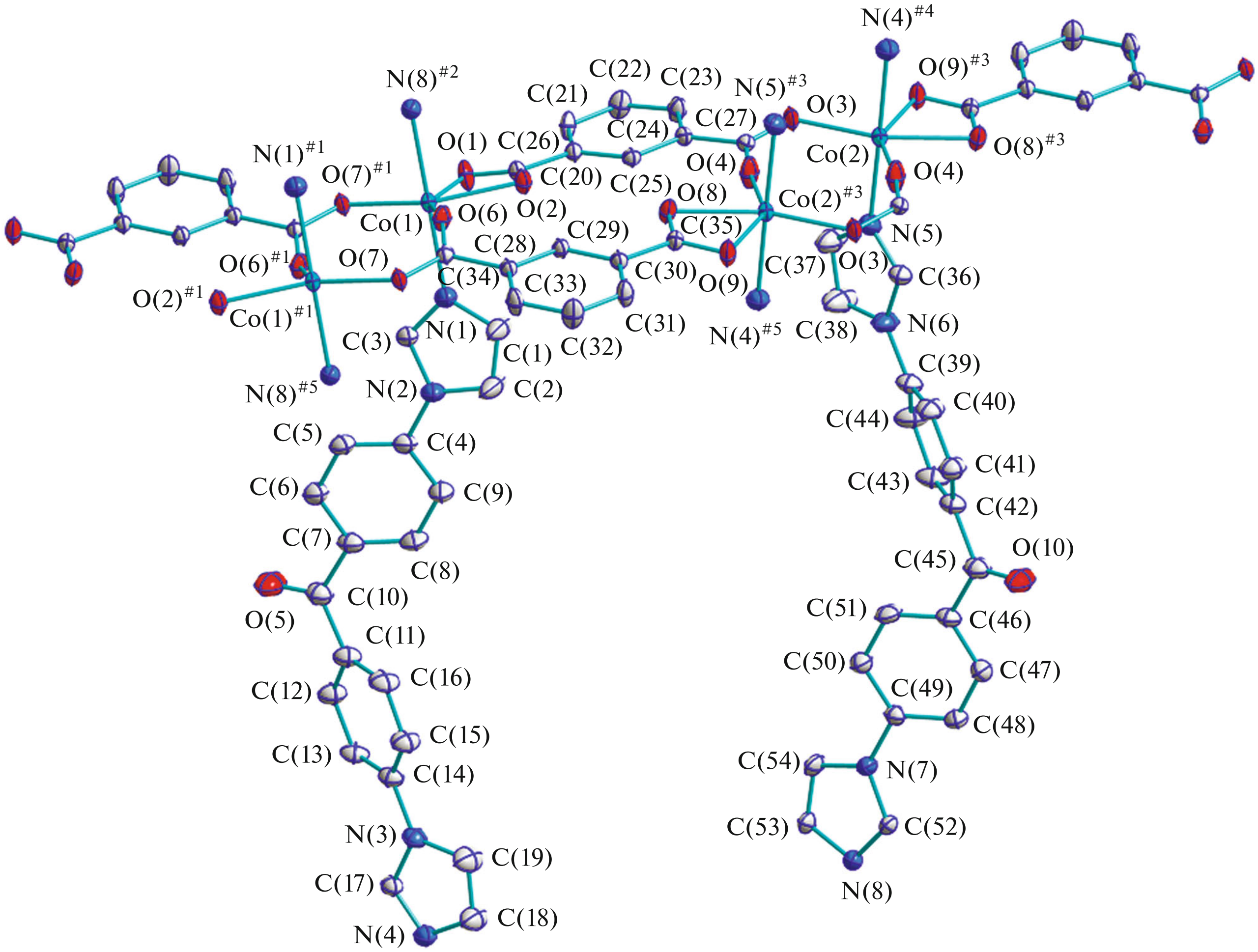

Fig. 1. ORTEP diagram showing the coordination environment of Co(II) atoms in **I**. The hydrogen atoms, DMF and lattice water molecules are omitted for clarity. Symmetry codes: $^{\#1}$ $-x, -y+1, -z$; $^{\#2}$ $x-1, y, z-1$; $^{\#3}$ $-x+1, -y, -z$; $^{\#4}$ $x, y-1, z-1$; $^{\#5}$ $1-x, 1-y, 1-z$.

nected nodes, respectively, which connect two Bipmo ligands and two Ipa^{2-} ligands. Each Ipa^{2-} and Bipmo unit serve as the bridging linker for the $\{Co\}_2$ units. The framework of **I** can be classified as 2D uninodal sql/Shubnikov tetragonal plane net (Fig. 2).

The asymmetric unit of **II** contains one Co^{2+} ions, one Ipa^{2-} ligand, one Bipmo ligand, and two lattice water molecules. As shown in Fig. 3, each Co^{2+} ion is six-coordinated with a slightly distorted $\{CoN_2O_4\}$ octahedral coordination geometry, which is coordinated by two nitrogen atoms from two Bipmo ligands, four oxygen atoms from two deprotonated Ipa^{2-} ligands. The Co(1)–O(1), Co(1)–O(2), Co(1)–O(3)$^{\#1}$, Co(1)–O(4)$^{\#1}$ are within the range of 2.0577(14)–2.3249(14) Å, and the bond lengths of Co(1)–N(1)$^{\#2}$, Co(1)–N(3) are 2.0588(15), 2.0600(14) Å, respectively ($^{\#1}$ $-x+1, y+1/2, -z+3/2$; $^{\#2}$ $-x+1, y-1/2, -z+3/2$), which are similar to the reported values for Co–O (1.937(5)–2.447(6) Å) and Co–N (2.007(5)–2.206(11) Å) [16–19].

The deprotonated carboxylic groups of H_2Ipa adopting μ^1-η^1:η^1 coordination mode link Co^{2+} ions to form a 1D chain. Neighboring chains are further linked by Bipmo ligands to furnish a 2D wave-like structure with ($4^4{\cdot}6^2$) topology along [0 0 1] direction (Figs. 4a, 4b). Interestingly, layers are threaded by the adjacent layers, thus resulting in a 2D→2D polythreading motif involving 2-fold interpenetrating sheets (Fig. 4).

In summary, two novel Co(II) CPs based on isophthalic acid (H_2Ipa), bis(4-(1*H*-imidazol-1-yl)phenyl)methanone (Bipmo) have been synthesized at different temperatures under solvothermal conditions. Complex **I** presents a 2D uninodal network with the point symbol $\{4^4{\cdot}6^2\}$ along [1, 1, 1] direction, while

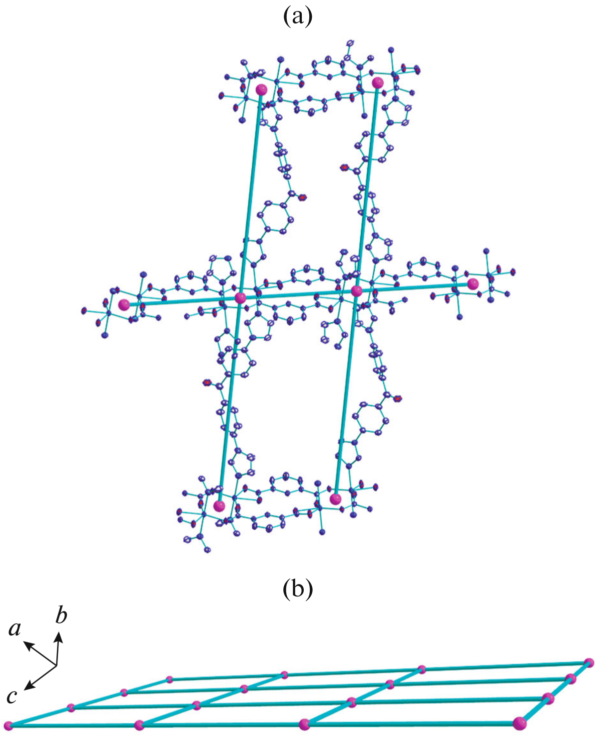

Fig. 2. View of the 2D network of **I**: along the *c*-axis (a), simplified net of **I** (b). The hydrogen atoms, DMF and lattice water molecules are omitted for clarity.

complex **II** shows two fold interpenetration with the same point symbol along [0 0 1] direction.

FUNDING

This research was supported by the Young Teacher Starting-up Research of Yuncheng University (YQ-2019022), the Priority Academic Program of Applied Chemistry (XK-2019057), and Scientific and Technological Innovation Programs of Higher Education Institutions in Shanxi Province (2019L0857).

CONFLICT OF INTEREST

The authors declare that they have no conflicts of interest.

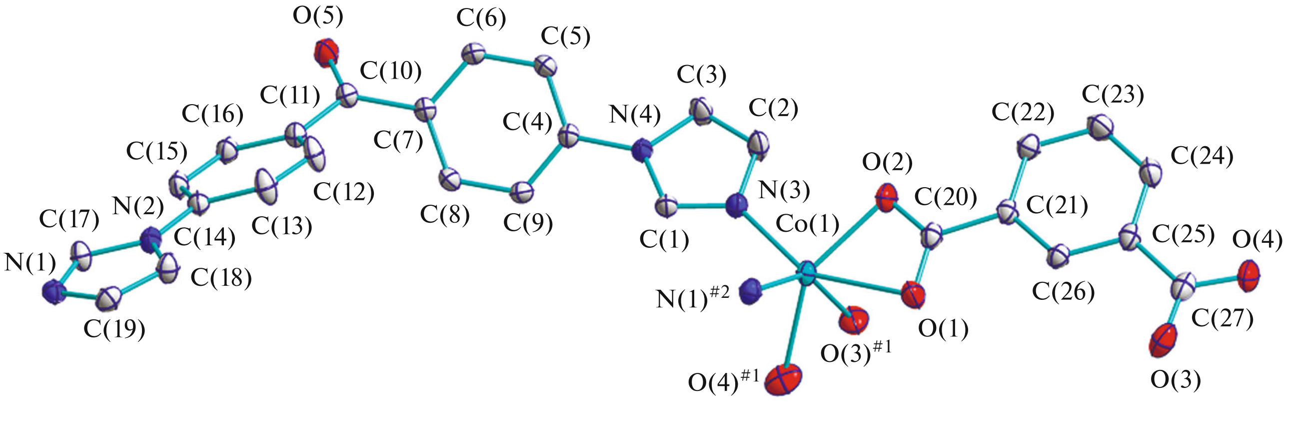

Fig. 3. ORTEP diagram showing the coordination environment of Co(II) atom in **II**. The hydrogen atoms and lattice water molecules are omitted for clarity. Symmetry codes: #1 $-x + 1, y + 1/2, -z + 3/2$; #2 $-x + 1, y - 1/2, -z + 3/2$.

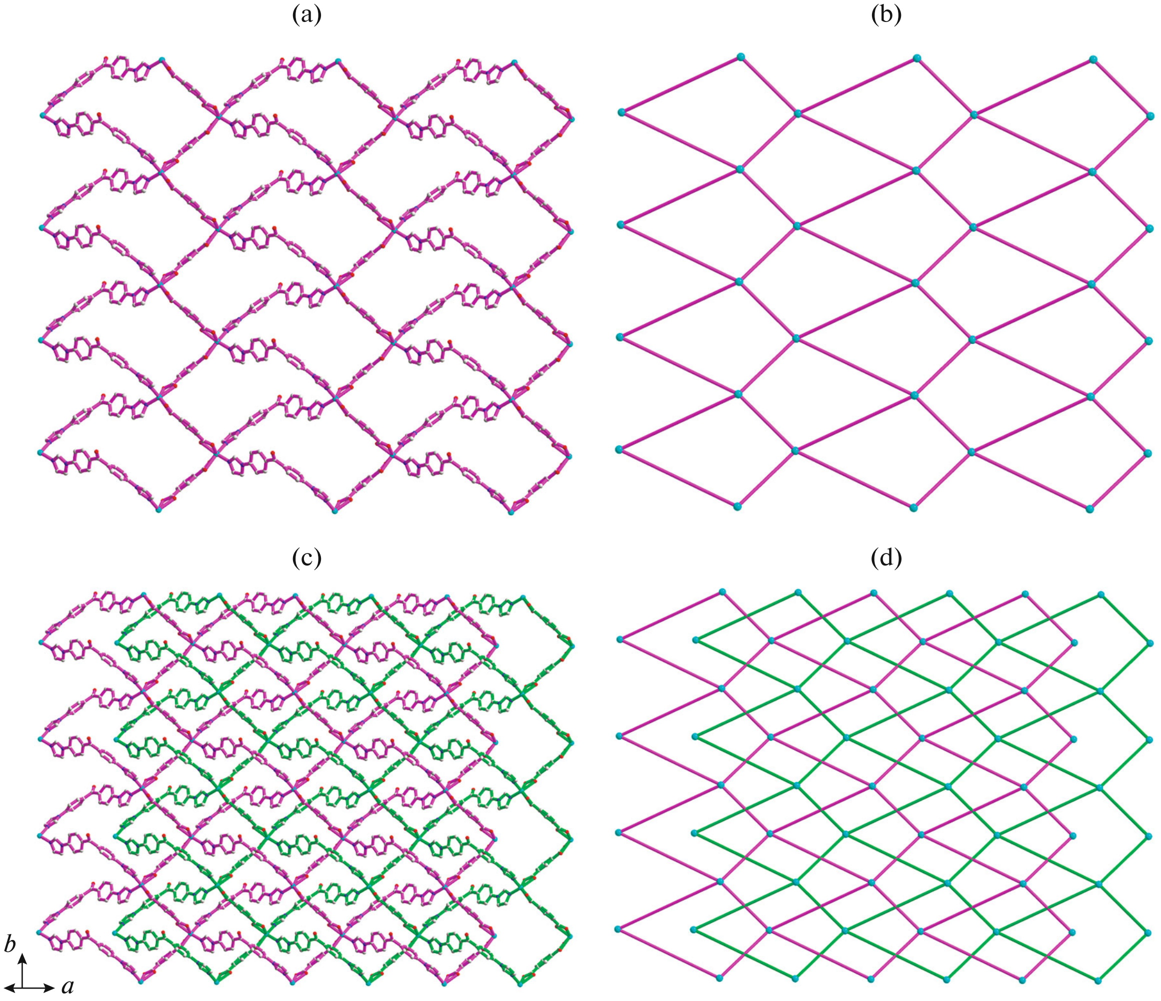

Fig. 4. View of the 2D network of **II**: one of the 2-fold interpenetrating network (a); 2D topology 4-connected framework with the Schläfli symbol ($4^4 \cdot 6^2$) (b); view of the 2-fold interpenetrating network (c); simplified 2-fold interpenetrating network (d).

REFERENCES

1. Chen, L., Tan, K., Lan, Y.Q., et al., *Chem. Commun.*, 2012, vol. 48, p. 5919.
2. Swamy, S.I., Bacsa, J., Jones, J.T.A., et al., *J. Am. Chem. Soc.*, 2010, vol. 132, p. 12773.
3. Corma, A., Garcia, H., and Llabres i Xamena, F.X., *Chem. Rev.*, 2010, vol. 110, p. 4606.
4. Stylianou, K.C., Warren, J.E., Chong, S.Y., et al., *Chem. Commun.*, 2011, vol. 47, p. 3389.
5. Ingram, C.W., Liao, L., Bacsa, J., et al., *Cryst. Growth Des.*, 2013, vol. 13, p. 1131.
6. Wang, G.F., *Rus. J. Coord. Chem.*, 2018, vol. 44, p. 540.
7. Rao, K.P., Higuchi, M., Duan, J., et al., *Cryst. Growth Des.*, 2013, vol. 13, p. 981.
8. Wang, P., Fan, R.-Q., Yang, Y.-L., et al., *CrystEngComm*, 2013, vol. 15, p. 4489.
9. Wang, G.-F., Sun, S.-W., Sun, H., et al., *Z. Naturforsch.*, B, 2020, vol. 75, p. 859.
10. Wang, G.-F., Zhang, X., Sun, S.-W., et al., *Z. Naturforsch.*, B, 2017, vol. 72, p. 257.
11. Wang, G.-F., Zhang, X., Liu, Z.-R., et al., *Z. Naturforsch.*, B, 2017, vol. 72, p. 83.
12. Wang, G.-F., Zhang, X., Sun, S.-W., et al., *Z. Naturforsch.*, B, 2016, vol. 71, p. 869.
13. *CrysAlis^{Pro}, Version 1.171.35.19,* Santa Clara: Agilent Technologies Inc., 2011.
14. Sheldrick, G.M., *SHELXTL-97*, Göttingen (Germany): Univ. of Göttingen, 1997.
15. Sheldrick, G.M., *Acta Crystallogr., Sect. A: Found. Crystallogr.*, 2008, vol. 64, p. 112.
16. Hou, X.-Y., Wang, X., Li, S.-N., et al., *Cryst. Growth Des.*, 2017, vol. 17, p. 3229.
17. Chen, Z., Gao, D.-L., Diao, C.-H., et al., *Cryst. Growth Des.*, 2012, vol. 12, p. 1201.
18. Ugale, B., Dhankhar, S.S., and Nagaraja, C.M., *Cryst. Growth Des.*, 2017, vol. 17, p. 3295.
19. Chen, Q., Chang, Z., Song, W.-C., et al., *Angew. Chem. Int. Ed.*, 2013, vol. 52, p. 11550.